Evaluation of allowable dynamic unbalance of a gyroscope rotor based on drift requirements

Nguyen Dinh Duy, Duong Dinh Quang*

Institute of Missile, Academy of Military Science and Technology, 17 Hoang Sam, Nghia Do, Hanoi, Vietnam.
*Corresponding author: ddquangmta@gmail.com
Received 05 Jun. 2026; Revised 18 Aug. 2026; Accepted 04 Sep. 2026; Published 16 Sep. 2026.
DOI: https://doi.org/10.54939/1859-1043.j.mst.FMC.2026.125-132

ABSTRACT

This study derives the equations of motion of a three-degree-of-freedom (3-DOF) gimballed gyroscope subjected to disturbance torques caused by residual dynamic unbalance of the rotor. The analytical results show that rotor dynamic unbalance induces forced high-frequency oscillations of the gyroscope axes and produces a steady drift component about the outer frame axis through reaction torques in the gimbal bearings. Based on the derived relationship between residual unbalance and drift rate, a drift-based criterion is proposed for estimating the maximum allowable residual unbalance of the rotor. Case studies for several gyroscope types show that the proposed criterion provides a practical upper tolerance for rotor balancing when the acceptance requirement is defined by allowable drift. Experimental residual-unbalance measurements for selected rotors are consistent with this drift-based tolerance.

Keywords: 3-DOF gyroscope; Dynamic unbalance; Residual unbalance; Drift rate; Rotor balancing.

1. INTRODUCTION

Material inhomogeneity, machining errors, manufacturing tolerances, and assembly deviations make it impossible to produce perfectly axisymmetric rotating components, including gyroscope rotors. As a result, a certain residual dynamic unbalance inevitably remains in the rotor. The influence of rotor unbalance on mechanical vibration, bearing loads, service life, and dynamic balancing requirements has been studied extensively [1-5]. For rotating machinery, residual unbalance is commonly associated with forced vibration, noise, increased bearing wear, and reduced bearing life [6, 7]. In a 3-DOF gimballed gyroscope, however, the problem is more critical because rotor unbalance can also degrade axis-holding accuracy and generate drift. Previous studies have mainly addressed the relationship between rotor dynamic unbalance and forced oscillations about the spin axis, active balancing methods [8, 9] and the use of genetic algorithms to optimize compensation-mass placement [10], whereas the analytical relationship between residual unbalance and gyroscope drift about the gimbal axes has not been sufficiently clarified. Practical manufacturing and testing of 3-DOF gyroscopes show that excessive residual rotor unbalance can lead to a significant drift rate. Therefore, this study aims to derive the relationship between residual dynamic unbalance and gyroscope drift and to use this relationship to define an allowable unbalance criterion consistent with the required operating accuracy. Although higher balancing accuracy generally improves gyroscope performance, excessively stringent balancing requirements increase production time, cost, and equipment demands. A drift-based allowable-unbalance criterion is therefore useful for selecting a technically adequate and economically practical balancing target for 3-DOF gyroscopes used in stabilization, orientation, and navigation systems.

2. PROBLEM

2.1. Motion of the gyroscope with an unbalanced rotor

To investigate the motion of a gyroscope with a dynamically unbalanced rotor, the following coordinate systems are introduced: Oxyz, attached to the gyroblock housing comprising the inner gimbal and the rotor; and $Ox_1y_1z_1$, attached to the rotor.

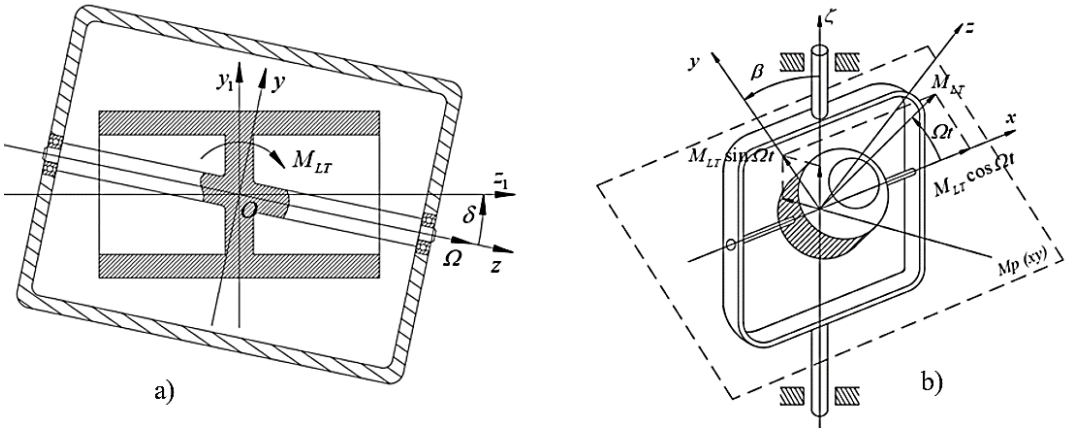


Figure 1. *Motion of a gyroscope with a dynamically unbalanced rotor.*

Assume that the principal inertia axis Oz_1 of the rotor deviates from its spin axis Oz by an angle δ. When the rotor spins about the Oz axis, the dynamic unbalance generates an inertial torque about the x-axis, which is perpendicular to the drawing plane and acts on the inner gimbal [1, 9-11].

$$M_{LT} = \left(C_0 - A_0\right)\Omega^2 \sin\delta\cos\delta \tag{1}$$

where C_0 and A_0 are the rotor moments of inertia about the principal inertia axes Oz_1 and Oy_1, respectively, and Ω is the rotor angular velocity. For a gyroscope rotor, C_0 is typically larger than A_0; therefore, $C_0 - A_0 > 0$. Consequently, the centrifugal moment of inertia M_{LT} tends to align the principal inertia axis Oz_1 with the spin axis Oz, forcing the rotor to rotate about the axis with the maximum moment of inertia. This torque periodically loads the spin-axis bearings at the rotational frequency Ω and may cause vibration and bearing degradation. As the rotor spins at angular velocity Ω, the torque M_{LT} also rotates in the xy plane at the same angular velocity.

Projecting the torque M_{LT} onto the *x* and *y* axes yields

$$M_x = M_{LT}\cos\Omega t;\; M_y = M_{LT}\sin\Omega t \tag{2}$$

Projecting torque M_y onto the ξ axis and normal direction to the outer frame plane, we obtain

$$M_\xi = M_{LT}\sin\Omega t\cos\beta;\; M_R = M_{LT}\sin\Omega t\sin\beta \tag{3}$$

The component MR is balanced by the reaction forces in the gimbal bearings. The components M_ξ and M_x are disturbance torques acting on the gyroscope about the outer and inner gimbal axes, respectively. Under these periodic torques, the rotor axis undergoes forced oscillations about the outer and inner gimbal axes at the rotational frequency Ω, with amplitudes governed by the level of rotor dynamic unbalance. Substituting these disturbance torques into the equations of motion of the gyroscope [1-3] gives

$$J_0\ddot{\alpha} + H\cos\beta_0\dot{\beta} = M_{LT}\sin\Omega t\cos\beta_0;\; A_0\ddot{\beta} - H\cos\beta_0\dot{\alpha} = -M_{LT}\sin\Omega t\sin\beta_0 \tag{4}$$

where A and C are the moments of inertia of the rotor; A_1, B_1, and C_1 are the moments of inertia of the inner gimbal (A_1 along the inner frame rotation axis, B_1 perpendicular to the inner frame plane, and C_1 along the rotor spin axis); and A_2 is the moment of inertia of the outer frame about its rotation axis.

Eliminating β from the system of equations (4) yields

$$\dddot{\alpha} + \frac{H^2\cos^2\beta_0}{A_0 J_0}\dot{\alpha} = \frac{M_{LT}}{J_0}\cos\beta_0\frac{A_0 + C}{A_0}\Omega\cos\Omega t \tag{5}$$

Letting

$$\frac{M_{LT}}{J_0}\cos\beta_0\frac{A_0+C}{A_0}\dot{\varphi}_0=h;\ \frac{H^2\cos^2\beta_0}{A_0J_0}=\omega_n^2$$

Equation (5) can be rewritten as

$$\ddot{\alpha}+\omega_n^2\dot{\alpha}=h\cos\Omega t \tag{6}$$

The general solution to equation (6) is

$$\dot{\alpha}=\dot{\alpha}_0\sin\omega_n t+\frac{\dot{\alpha}_0}{n}\cos\omega_n t-\frac{h}{n^2-\Omega^2}\frac{\Omega}{n}\cos\omega_n t+\frac{h}{n^2-\Omega^2}\cos\Omega t \tag{7}$$

The first three terms of solution (7) represent the free oscillations of the gyroscope. Their amplitudes decay rapidly even in the presence of small damping moments. In the steady state, only the forced oscillations of the Oz axis remain

$$\dot{\alpha}=\frac{h}{\omega_n^2-\Omega^2}\cos\Omega t=\frac{M_{LT}\left(A_0+C\right)}{\Omega\left(C^2\cos^2\beta_0-A_0J_0\right)}\cos\beta_0\cos\Omega t \tag{8}$$

Integrating expression (8) and applying the corresponding initial conditions yields the angular displacement of the gyroscope about the outer and inner gimbal axes

$$\alpha=\frac{M_{LT}\left(A_0+C\right)}{\Omega^2\left(C^2\cos^2\beta_0-A_0J_0\right)}\cos\beta_0\sin\Omega t;\ \beta=-\frac{M_{LT}\left(C\cos^2\beta_0+J_0\right)}{\Omega^2\left(C^2\cos^2\beta_0-A_0J_0\right)}\cos\Omega t \tag{9}$$

The amplitudes of these forced oscillations about the outer and inner frame axes are defined as

$$\alpha_A=\frac{M_{LT}\left(A_0+C\right)\cos\beta_0}{\Omega^2\left(C^2\cos^2\beta_0-A_0J_0\right)};\ \beta_A=\frac{M_{LT}\left(C\cos^2\beta_0+J_0\right)}{\Omega^2\left(C^2\cos^2\beta_0-A_0J_0\right)} \tag{10}$$

Taking the time derivative of expression (9) yields

$$\ddot{\alpha}=-\frac{M_{LT}\left(A_0+C\right)}{\left(C^2\cos^2\beta_0-A_0J_0\right)}\cos\beta_0\sin\Omega t \tag{11}$$

The ratio between the forced oscillation amplitudes of the inner and outer frame axes is expressed as

$$k=\frac{\beta_A}{\alpha_A}=\frac{C\cos^2\beta_0+J_0}{C\cos\beta_0+A_0\cos\beta_0} \tag{12}$$

In the steady state, the axis of the unbalanced rotor undergoes forced oscillations with amplitudes αA and βA at a frequency equal to the rotor spin frequency Ω. The motion traces an elliptical cone in space, elongated along the angular deviation in the β coordinate. This behavior is analogous to the free nutation of a gimballed gyroscope following an instantaneous torque impulse. In this case, the reaction torque in the gimbal bearings associated with the oscillation of the gyroscope about the Oz axis is determined by [1]:

$$M_R=\left(A_2+C_1\right)\ddot{\alpha}tg\beta_0 \tag{13}$$

Under the influence of the reaction torque in the gimbal bearings, the gyroscope undergoes continuous precessional motion about the outer frame axis with a velocity of

$$\left(\dot{\alpha}\right)_{tb}=\frac{M_R\sin\alpha}{\theta_1}\approx\frac{M_{z0}^R\alpha}{H\cos\beta_0} \tag{14}$$

Substituting expression (13) into (14) yields

$$\left(\dot{\alpha}\right)_{tb} = \frac{\left(A_2 + C_1\right)\ddot{\alpha}\alpha tg\beta_0}{H\cos\beta_0} \tag{15}$$

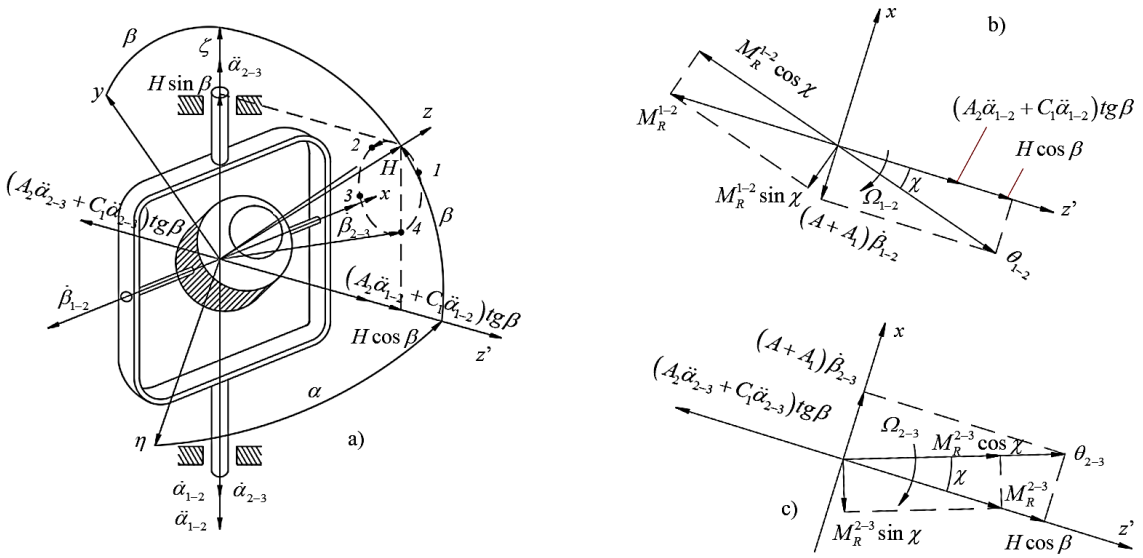


Figure 2. *Nutation motion of the gyroscope [1].*

Substituting αA from expression (10) and the corresponding terms from expression (11) into expression (15), and solving with respect to the integration constants, gives

$$\left(\dot{\alpha}\right)_{tb} = -\frac{M_{LT}^2}{C\Omega^3}\frac{\left(A_2 + C_1\right)\left(A_0 + C\right)^2}{\left(C^2\cos^2\beta_0 - A_0 J_0\right)^2}\sin\beta_0\left(\frac{1}{2} - \frac{1}{2}\cos 2\Omega t\right)$$

The constant component of the precessional velocity, i.e., the drift rate caused by rotor dynamic unbalance, is then obtained as

$$\left(\dot{\alpha}\right)_{tb}^{0} = -\frac{M_{LT}^2}{2C\Omega^3}\frac{\left(A_2 + C_1\right)\left(A_0 + C\right)^2}{\left(C^2\cos^2\beta_0 - A_0 J_0\right)^2}\sin\beta_0 \tag{16}$$

Substituting the expressions for A_0 and J_0 into (16) yields

$$\left(\dot{\alpha}\right)_{tb}^{0} = \frac{M_{LT}^2}{2C\Omega^3}\frac{\left(A_2 + C_1\right)\left(A + A_1 + C\right)^2\sin\beta_0}{\left\{\left(A + A_1\right)\left[A_2 + \left(A + B_1\right)\cos^2\beta_0 + C_1\sin^2\beta_0\right] - C^2\cos^2\beta_0\right\}^2} \tag{17}$$

Let m be the mass of the correction weight required to fully balance the rotor, R- the radius designating the position of the added weight, and L - the distance between the two correction planes. We establish

$$\left(\dot{\alpha}\right)_{tb}^{0} = \frac{M_{LT}^2}{2C\Omega^3}\frac{\left(A_2 + C_1\right)\left(A + A_1 + C\right)^2\sin\beta_0}{\left\{\left(A + A_1\right)\left[A_2 + \left(A + B_1\right)\cos^2\beta_0 + C_1\sin^2\beta_0\right] - C^2\cos^2\beta_0\right\}^2} \tag{18}$$

where U denotes the equivalent residual dynamic unbalance of the rotor. If U is interpreted as a dynamic couple unbalance, its unit is kg·m²; for comparison with balancing-machine outputs, the corresponding residual unbalance is reported below in g·mm. Substituting expression (18) into expression (17) yields

$$\left(\dot{\alpha}\right)_{tb}^{0}=\frac{D^{2}\Omega}{2C}\frac{\left(A_{2}+C_{1}\right)\left(A+A_{1}+C\right)^{2}\sin\beta_{0}}{\left\{\left(A+A_{1}\right)\left[A_{2}+\left(A+B_{1}\right)\cos^{2}\beta_{0}+C_{1}\sin^{2}\beta_{0}\right]-C^{2}\cos^{2}\beta_{0}\right\}^{2}} \tag{19}$$

Formula (19) provides a direct basis for estimating the allowable residual dynamic unbalance of the rotor from the structural parameters and drift-accuracy requirements of the gyroscope.

$$D=\frac{\left\{\left(A+A_{1}\right)\left[A_{2}+\left(A+B_{1}\right)\cos^{2}\beta_{0}+C_{1}\sin^{2}\beta_{0}\right]-C^{2}\cos^{2}\beta_{0}\right\}}{\left(A+A_{1}+C\right)}\sqrt{\frac{2C\left(\dot{\alpha}\right)_{tb}^{0}}{\Omega\left(A_{2}+C_{1}\right)\sin\beta_{0}}} \tag{20}$$

2.2. Rotor dynamic balancing and dynamic-unbalance requirements

To minimize structural vibration and improve operational life and accuracy, gyroscope rotors must be dynamically balanced [12-15]. According to ISO 1940-1 [16], high-precision gyroscope rotors are commonly associated with balance quality grade G0.4. This standard defines allowable residual unbalance mainly as a function of rotor mass and operating speed.

However, strictly achieving such standardized limits in production can be difficult because it requires high-precision balancing equipment, careful process control, and considerable processing time.

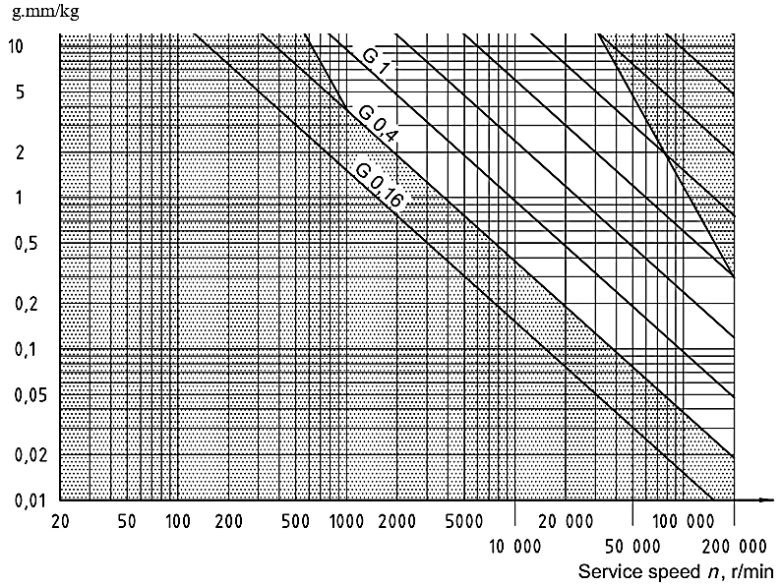


Figure 3. *Residual unbalance requirements for various rotor types according to ISO 1940-1.*

Based on ISO 1940-1 and the operating profiles of the B72 gyroscope (maximum speed 27,000 rpm), B87 gyroscope (maximum speed 90,000 rpm), and 9B861 gyroscope (maximum speed 20,000 rpm), the corresponding ISO-based allowable residual unbalances were calculated as 18.0×10^{-3} g·mm, 2.97×10^{-3} g·mm, and 7.64×10^{-3} g·mm, respectively. These limits are very stringent and may be difficult to achieve under ordinary production conditions without specialized balancing infrastructure.

3. RESULTS AND DISCUSSION

The derived model indicates that the precessional drift of a gyroscope with a dynamically unbalanced rotor is initiated by the centrifugal disturbance torque generated during high-speed rotation. This torque excites forced oscillations of the gimbal system, while the reaction moments generated in the gimbal bearings produce a steady drift component about the outer frame axis.

The mean velocity of this precession is governed by expression (19). In general, gyroscope drift is linearly related to disturbance torques such as bearing-friction torque, lead-wire restraint torque, and torques caused by non-uniform structural stiffness [1, 2]. In contrast, expression (19) indicates that, for fixed structural parameters and operating speed, the drift component caused by rotor dynamic unbalance increases with the square of the residual unbalance. This result emphasizes the strong influence of rotor balancing accuracy on gyroscope performance.

Table 1. *Technical parameters of the investigated gyroscopes.*

Parameter		**Symbol**	**Value**		
			B72	**B87**	**9B861**
Moment of inertia, kg·m²	Rotor	A	0.184×10^{-4}	0.9×10^{-5}	0.37×10^{-5}
		C (spin axis)	0.185×10^{-4}	1.1×10^{-5}	0.375×10^{-5}
	Inner frame	A_1 (rotation axis)	0.53×10^{-5}	0.33×10^{-5}	0.085×10^{-5}
		B_1	0.87×10^{-5}	0.54×10^{-5}	0.093×10^{-5}
		C_1	0.44×10^{-5}	0.59×10^{-5}	0.131×10^{-5}
	Outer frame	A_2 (rotation axis)	0.54×10^{-5}	0.86×10^{-5}	0.368×10^{-5}
Rotor mass, g		m	132	70	20
Rotor dimensions (Diameter × length), mm		Φ x H	32.5 × 27	30 × 22	25.2 × 27.8
Operating velocity, rpm		ω	27,000	90,000	20,000
Max allowable outer frame drift		Δα	±1°/30 s	±2°/15 s	±5°/20 s

Using formula (19), the maximum allowable residual unbalance values for the B72, B87, and 9B861 gyroscopes based on drift requirements are evaluated as 2.5 g·mm, 1.6 g·mm, and 1.4 g·mm, respectively.

It should be noted that physical gyroscope drift is a multivariate phenomenon affected by bearing friction, lead-wire torque, structural elasticity, support clearances, and other disturbance sources. The above calculations adopt a conservative allocation in which the total permissible drift is assigned to rotor dynamic unbalance, thereby defining an upper tolerance for manufacturing when drift is used as the acceptance criterion.

To examine the practical applicability of the drift-based criterion, residual-unbalance measurements were carried out for the B72 and B87 gyroscope rotors.



a) b)

Figure 4. *Residual-unbalance measurement for the B72 (a) and B87 (b) gyroscope rotors.*

Table 2. *Comparison of rotor residual-unbalance limits and measured values.*

Gyroscope type	Residual dynamic unbalance (g·mm)		
	ISO-1940 standard limit	**Drift-based requirement**	**Actual measured result**
B72	18.0×10^{-3}	2.5	0.6
B87	2.97×10^{-3}	1.6	0.25
9B861	7.64×10^{-3}	1.4	-

The measured residual unbalance values of the B72 and B87 rotors are much higher than the ISO 1940-1 G0.4 limits but remain well below the drift-based allowable limits. This indicates that the ISO-based requirement is significantly more stringent than necessary when the acceptance criterion is defined solely by allowable gyroscope drift. Therefore, the drift-based criterion may serve as a practical manufacturing tolerance, whereas ISO 1940-1 can be regarded as a stricter reference target. Because the experimental data report residual unbalance rather than directly measured drift rates under controlled unbalance levels, these measurements should be interpreted as supporting the practical applicability of the proposed criterion rather than fully validating the analytical model.

Consequently, combining the proposed drift-based analytical criterion with the ISO 1940-1 reference can provide a useful tolerance envelope for balancing requirements: ISO 1940-1 defines a stringent precision target, while the drift-based criterion defines an application-specific upper limit linked to operational accuracy.

4. CONCLUSIONS

From the theoretical modeling and comparative evaluation presented in this study, the following conclusions can be drawn:

- An analytical framework was developed for evaluating the allowable residual dynamic unbalance of a 3-DOF gimballed gyroscope rotor based on drift requirements. The derived equations show that rotor dynamic unbalance excites forced high-frequency oscillations of the gyroscope axes and can generate a steady drift component about the outer frame axis through reaction torques in the gimbal bearings.

- The analytical relationship indicates that, under fixed structural and operating conditions, the drift component associated with rotor dynamic unbalance increases with the square of the residual unbalance and depends on the inertia parameters of the rotor and gimbal assemblies.

- Application of the proposed criterion to the B72, B87, and 9B861 gyroscopes produced drift-based allowable residual-unbalance limits that are less stringent than the corresponding ISO-based balancing limits. This suggests that the proposed method can provide a practical upper tolerance for rotor balancing when the design acceptance criterion is defined by allowable gyroscope drift.

- Measurements of residual unbalance for the B72 and B87 rotors were below the calculated drift-based limits, supporting the practical applicability of the proposed approach. Further validation should include direct drift-rate measurements under controlled residual-unbalance levels. The model also indicates that reducing the initial angular misalignment of the gyroscope axes can help suppress the drift component associated with rotor dynamic unbalance.

REFERENCES

[1]. D. S. Pelpor, "*Gyroscopic Systems. Theory of Gyroscopes and Gyrostabilizers*", Vysshaya Shkola Publishing House, Moscow, (1986). (in Russian)

[2]. N. Lysov and A. A. Lysova, "*Theory of Gyroscopic Stabilizers: A Textbook*", SUSU Publishing Center, Chelyabinsk, p. 117, (2009). (in Russian)

[3]. R. N. Arnold, "*Gyrodynamics and its Engineering Applications*", Academic Press, p. 485., (2014).

[4]. X. Hou, E. Wang, H. Cao, Y. Zhu and K. Qi, "*Research on dynamic balance adjustment method of single braced frame gyroscope rotor*", MATEC Web of Conferences, (2019).
[5]. L. Huang, Z. Wu and K. Wang, "*Indirect measurement of rotor dynamic unbalance for control moment gyroscopes via gimbal disturbance observer*", Sensors, (2018).
[6]. Vu Van Thung, "*Research on the Influence of Several Structural and Dynamic Parameters on the Accuracy of a 3-DOF Inner Gimbal Gyroscope for Missile Infrared Homing Heads*", PhD Thesis, Hanoi, (2012). (in Vietnamese)
[7]. Nguyen Dinh Duy, Nguyen Phu Thang and Pham Khac Lam, "*Investigation into the Influence of Rotor Dynamic Unbalance on the Accuracy of B-72 Missile Gyroscopes*", Journal of Military Science and Technology, No. 50, (2017). (in Vietnamese)
[8]. Soo-Hun Lee, Bong-Suk Kim, Jong-Duck Moon and Do-Hyung Kim, "*A study on active balancing for rotating machinery using influence coefficient method*", 2005 International Symposium on Computational Intelligence in Robotics and Automation, Espoo, pp. 659–664, (2005). DOI: 10.1109/CIRA.2005.1554352.
[9]. Pan, Xin Xie, Zhen Lu, Juan Wu, Haiqi Gao, Jinji Jiang and Zhinong, "*Novel liquid transfer active balancing system for hollow rotor of high-speed rotating machinery*", Applied Sciences, (2019).
[10]. Q. Song, Z. Wang and L. Liang, "*Optimization method based on genetic algorithm for the mass compensation of the rotor on-line dynamic balance system*", IOP Conference Series: Materials Science and Engineering, Vol. 1242, p. 012036, (2022). DOI: 10.1088/1757-899X/1242/1/012036.
[11]. H. Goldstein, C. P. Poole Jr. and J. L. Safko, "*Classical Mechanics*".
[12]. L. D. Landau and E. M. Lifshitz, "*Mechanics: Volume 1 of Course of Theoretical Physics*".
[13]. M. V. Barkan et al., "*Modern Methods and Tools for Balancing Machines and Instruments*", edited by V. A. Shchepetilnikov, Mashinostroenie, Moscow, 232 p., (1986). (in Russian)
[14]. M. E. Levit, Yu. A. Agofonov, L. D. Vaingortin et al., "*Balancing Handbook*", edited by M. E. Levit, Mashinostroenie, Moscow, 464 p., (1992). (in Russian)
[15]. "*ISO 1940-1:2003. Mechanical vibration — Balance quality requirements for rotors in a constant (rigid) state*", (2003).
[16]. "*GOST 22061—76. Machines and Technological Equipment. System of Balancing Accuracy Classes. Basic Principles*", (1976). (in Russian)

TÓM TẮT

Xác định giới hạn mất cân bằng động cho phép của rô to con quay trên cơ sở yêu cầu về độ trôi

Bài báo trình bày kết quả xây dựng phương trình chuyển động của con quay ba bậc tự do chịu tác động của mô men nhiễu do mất cân bằng động còn dư của rô to. Phân tích nghiệm của hệ phương trình cho thấy mất cân bằng động của rô to không chỉ gây dao động cưỡng bức tần số cao của các trục con quay mà còn có thể tạo thành phần trôi quanh trục khung ngoài thông qua mô men phản lực trong ổ đỡ khung các đăng. Trên cơ sở quan hệ giải tích giữa lượng mất cân bằng còn dư và tốc độ trôi, bài báo đề xuất tiêu chí xác định giới hạn mất cân bằng động cho phép của rô to theo yêu cầu độ trôi trong thời gian làm việc. Các tính toán cho một số loại con quay cho thấy tiêu chí theo độ trôi có thể được sử dụng như một giới hạn công nghệ thực tế, trong khi tiêu chuẩn ISO 1940-1 đóng vai trò mục tiêu cân bằng nghiêm ngặt hơn. Kết quả đo mất cân bằng còn dư trên một số rô to con quay phù hợp với giới hạn tính theo tiêu chí độ trôi, qua đó hỗ trợ khả năng áp dụng thực tế của phương pháp đề xuất.

Từ khóa: Con quay ba bậc tự do; Mất cân bằng động; Mất cân bằng còn dư; Độ trôi; Cân bằng rô to.